DOI: 10.1002/ejic.200900004

Structure, Spectral and Magnetic Properties of 3-(*p*-Pyridyl)-1,5-diphenylverdazyl (*p*-PyV) and the Binuclear Copper(II) Radical Complex $[Cu_2(OCOCH_3)_4(p\text{-PyV})_2]$

Anastasiya V. Yakovenko,[a] Sergey V. Kolotilov,[a] Olivier Cador,[b] Stéphane Golhen,[b] Lahcène Ouahab,*[b] and Vitaly V. Pavlishchuk*[a]

Keywords: Radicals / Copper / X-ray diffraction / EPR spectroscopy / Magnetic properties

3-(*p*-Pyridyl)-1,5-diphenylverdazyl (*p*-PyV) and its binuclear copper(II) complex $[Cu_2(OCOCH_3)_4(p\text{-PyV})_2]$ have been synthesized and structurally characterized. The magnetic behavior of a single crystal of *p*-PyV and $[Cu_2(OCOCH_3)_4(p\text{-PyV})_2]$ have been studied by magnetic susceptibility measurements in the temperature range 2–300 K and by ESR spectroscopy. Data fitting for *p*-PyV using the singlet-triplet equilibrium model revealed the existence of antiferromagnetic interactions in the radical crystal lattice. The exchange interactions between the copper(II) ion and *p*-PyV in $Cu_2(OCOCH_3)_4(p\text{-PyV})_2$ were found to be negligibly small compared to the strong intramolecular copper–copper antiferromagnetic interaction. Intermolecular antiferromagnetic coupling between *p*-PyV molecules was detected in the crystal lattice of complex.

Introduction

The magnetic properties of free radicals and their complexes with paramagnetic metal ions have been attracting attention in the search for compounds for new molecular magnetic materials. Free radicals such as nitronyl nitroxides,[1] imino nitroxides,[2] and semiquinones[3] are considered to be promising candidates for this purpose. Several examples of free radicals[4] and metal-radical complexes[1c–1f] possessing the properties of molecular or single-chain magnets have been reported. The chemistry of verdazyl radicals[5] and their coordination compounds with metal ions has been studied extensively in recent years.[6] The interest in this class of free radicals lies in their comparatively high stability,[5b] the intriguing magnetic properties of some examples,[7] and the possibility of obtaining radicals possessing different functional groups that are capable of coordinating to metal ions.[8] Although the coordination chemistry of verdazyl radicals with paramagnetic metal ions is not as extensive as that of paramagnetic metal complexes with other classes of free radicals,[1–3] it was expected that strong ferromagnetic coupling between the verdazyl radical and paramagnetic metal ion may arise. The magnitude of such coupling may even have one of the highest exchange integrals (*J*) of all known metal-radical complexes.[9] However, the majority of metal-verdazyl complexes studied so far are mononuclear ones, and the attention of researchers has focused solely on metal-radical coupling.

Mukai et al.[10] have studied the magnetic properties of a bulk sample of *p*-PyV and suggested the existence of spin frustration for this radical. However, these authors could not reach a reliable conclusion since the crystal structure of this compound was not determined. Thus, this radical was chosen as the object of our study due to its possibly nontrivial magnetic properties and its capability to coordinate to metal ions through the nitrogen atom of the pyridyl group.

Dimeric copper(II) acetate, which possesses strong antiferromagnetic exchange between the two copper atoms,[11] is one of the most studied binuclear magnetic systems. It is also a suitable model for studying the effect of metal-radical coupling on the overall magnetic properties of multispin systems containing an organic radical and a polynuclear complex. The properties of several binuclear copper(II) carboxylates with nitronyl nitroxide ligands were reported recently,[12] and it was found that the magnetic interactions between the copper(II) ion and radical in the complex containing bridging benzoates with nitronyl nitroxides in the *para*- and *meta*-positions of the phenyl ring were negligible.[12a] A similar result was obtained in the case of dimeric copper(II) acetate with (*p*-pyridyl)nitronyl nitroxide as an

[a] L. V. Pisarzhevskii Institute of Physical Chemistry of the National Academy of Sciences of the Ukraine,
Prospekt Nauki 31, Kiev 03028, Ukraine
Fax: +380-44-525-62-16
E-mail: shchuk@inphyschem-nas.kiev.ua
[b] Equipe Organométalliques et Matériaux Moléculaires, Sciences Chimiques de Rennes, UMR UR1-CNRS 6226, Université de Rennes 1,
Campus de Beaulieu, 35042 Rennes Cedex, France
Fax: +33-2-23236840
E-mail: ouahab@univ-rennes1.fr

apical neutral ligand.[12b] To study the influence of the nature of the radical on the magnetic coupling between the radical and copper(II) ion, we synthesized binuclear copper(II) acetate with 3-(*p*-pyridyl)-1,5-diphenylverdazyl radicals (*p*-PyV) coordinated to the copper(II) atoms. Herein we report the crystal structure of *p*-PyV and the magnetic properties of a single crystal of this radical as well as the structure and magnetic properties of $[Cu_2(OCOCH_3)_4(p\text{-}PyV)_2]$.

Results and Discussion

Synthesis and Structure

3-(*p*-Pyridyl)-1,5-diphenylverdazyl (*p*-PyV) was obtained by cyclization of 3-(*p*-pyridyl)-1,5-diphenylformazane with formaldehyde in a basic medium.[10] Substitution of the two axial water molecules in paddle-wheel copper acetate by *p*-PyV in methanol resulted in the formation of $[Cu_2(OCOCH_3)_4(p\text{-}PyV)_2]$.

The crystal structures of *p*-PyV and $[Cu_2(OCOCH_3)_4(p\text{-}PyV)_2]$ were studied by X-ray analysis; selected labeled ORTEP drawings are shown in Figures 1 and 3, respectively. Selected bond lengths and angles for *p*-PyV and $[Cu_2(OCOCH_3)_4(p\text{-}PyV)_2]$ are listed in Tables 1 and 2, respectively.

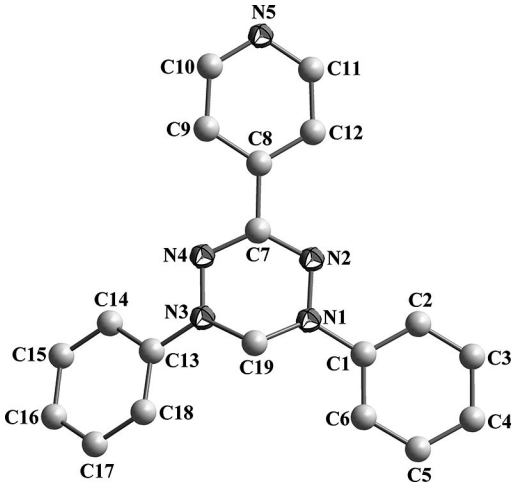

Figure 1. Molecular structure of *p*-PyV. Hydrogen atoms have been omitted for clarity.

Table 1. Selected bond distances [Å] and angles [°] for *p*-PyV.

N3–N4	1.356(2)	N3–N4–C7	114.16(14)
C7–N4	1.340(2)	N4–C7–N2	127.12(16)
C7–N2	1.339(2)	C7–N2–N1	114.74(14)
N2–N1	1.348(2)	N3–N4–C7	114.16(14)
C19–N1	1.445(2)	Φ1–Φ2	42.75(7)
C19–N3	1.455(2)	Ver–Φ2	35.19(9)
N3–N4	1.356(2)	Ver–Φ1	7.63(14)
N2–N1–C19	116.78(9)	Ver–Py	9.40(13)
N1–C19–N3	106.55(9)	Py–Φ1	3.31(13)
C19–N3–N4	116.36(8)	Py–Φ2	44.45(7)

Table 2. Selected bond distances [Å] and angles [°] for $[Cu_2(OCOCH_3)_4(p\text{-}PyV)_2]$.

	Molecule A[a]	Molecule B[a]
Cu1–Cu1^{i}	2.6622(12)	2.6362(12)
Cu1–O1	1.980(4)	1.955(3)
Cu1–O2	1.949(3)	1.963(3)
Cu1–O3	1.968(4)	1.973(3)
Cu1–O4	1.956(3)	1.969(3)
Cu1–N5	2.206(4)	2.179(4)
N1–N2	1.352(5)	1.346(5)
C7–N2	1.338(5)	1.337(5)
C7–N4	1.337(6)	1.328(6)
N4–N3	1.352(5)	1.356(5)
C19–N3	1.433(6)	1.442(6)
C19–N1	1.431(6)	1.440(6)
N1–N2–C7	113.7(4)	114.6(4)
N2–C7–N4	127.1(5)	127.4(5)
C7–N4–N3	114.1(4)	115.0(4)
N4–N3–C19	117.5(4)	119.5(4)
N3–C19–N1	106.6(4)	107.8(4)
C19–N1–N2	117.6(4)	119.9(4)
O1–O3/O2–O4	89.96(15)	89.76(15)
O2–Cu1–O4	167.22(15)	168.09(14)
O2–Cu1–O3	88.14(16)	89.74(15)
O4–Cu1–O3	89.94(16)	88.56(15)
O2–Cu1–O1	88.64(15)	90.39(17)
Φ1–Φ2	54.12(14)	32.44(22)
Ver–Φ1	29.76(18)	17.81(23)
Ver–Φ2	44.49(16)	20.46(23)
Ver–Py	2.34(30)	7.04(24)
Py–Φ2	46.00(17)	17.72(27)
Py–Φ1	31.46(20)	15.34(27)
O4–Cu1–O1	90.47(15)	88.80(16)
O3–Cu1–O1	167.19(14)	167.77(14)
C11–N5–Cu1	123.9(3)	121.1(3)
C10–N5–Cu1	118.7(3)	121.6(3)
C20–O1–Cu1^{i}	122.7(4)	126.2(4)
C22–O2–Cu1^{i}	120.5(3)	125.2(3)
C20–O3–Cu1	125.0(4)	120.8(3)
C22–O4–Cu1	127.5(4)	120.8(3)

[a] i: 2 – *x*, 1 – *y*, 1 – *z* for A and –*x*, –*y*, –*z* for B.

The molecular structure of *p*-PyV (Figure 1) reveals similar features to those of other 1,3,5-triarylverdazyls.[10,13] Thus, the heterocyclic ring in *p*-PyV has an unsymmetrical boat conformation with the four nitrogen atoms lying almost in one plane (Ver). Atoms C19 and C7 are located 0.606(3) and 0.106(3) Å, respectively, out of this plane. The presence of sp^3-hybridized C19 results in noticeable differences in C–N bond lengths involving atoms C7 and C19 in the heterocyclic ring (Table 1) and confirms that the ring is not conjugated. Nevertheless, the pyridyl ring (Py) and the phenyl ring attached to N1 (called Φ1) are conjugated as they fit the plane containing atoms C1, N1, N2, C7, and C8 [the largest deviation from the mean plane is 0.0197(10) Å for C7] whereas the distance of C5 to this plane is 0.116(3) Å (the largest distance among these atoms). The Py and phenyl rings attached to N3 (Φ2) are not conjugated, as can be concluded from the much higher deviations of the corresponding atoms from the mean plane containing C13, N3, N4, C7, and C8. The angles between the plane formed by the four nitrogen atoms of verdazyl (Ver) and the phenyl rings attached to N3 (Φ2) and N1

(Φ1), are 35.19(9)° and 7.63(14)°, respectively, while the angle between the Ver plane and the Py plane is 9.40(13)°.

Two *p*-PyV molecules are packed in the crystal lattice, with a shortest distance between the nitrogen atoms of adjacent verdazyls of 3.515(3) Å (between atoms N2 and N2′). The two parts of this dimer are related by an inversion center. Furthermore, the distances between the pyridyl ring (Py) and Φ1 substituents in a dimer are relatively short (Figure 2), with a mean interatomic distance of 3.865(1) Å. These rings are also quasi-coplanar, with an angle between the mean planes of 3.31(13)°. The two rings are displaced with respect to each other. Figure 3 shows the ring-centroid vectors[14] (their norms correspond to centroid-mean plane distances), which point slightly out of the rings. Although there are no contacts shorter than 3.5 Å, this small overlap probably contributes to stabilizing the dimers in the crystal lattice. No other significantly short distances between *p*-PyV molecules can be found.

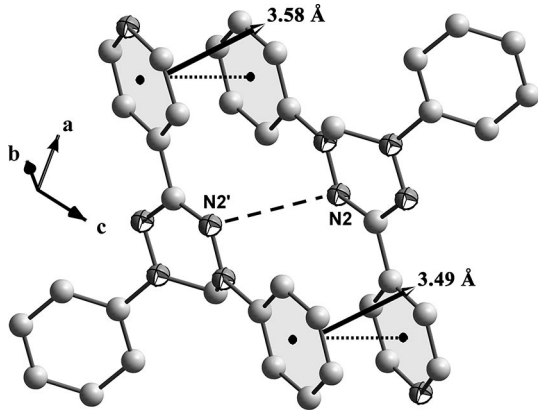

Figure 2. View of a dimer showing the shortest interatomic distance (dashed line) between two nitrogen atoms belonging to two molecules [3.515(3) Å]. The vectors correspond to ring-centroid vectors and the dotted line to the centroid-centroid distances [3.865(1) Å].

$[Cu_2(OCOCH_3)_4(p\text{-PyV})_2]$ crystallizes as two independent centrosymmetric binuclear complexes labeled A and B with the same labeling scheme for the verdazyl part as used for *p*-PyV (Figure 3). The binuclear core of these complexes possesses a "paddlewheel" geometry similar to $[Cu_2(OCOCH_3)_4(H_2O)_2]$,[15] where two copper(II) ions are connected by four acetate anions acting in a $\mu(\eta_1\text{-O1},\eta_1\text{-O3})$ and $\mu(\eta_1\text{-O2},\eta_1\text{-O4})$ bridging coordination mode. The distance between copper(II) ions [2.6622(12) and 2.6362(12) Å] and the angles Cu–O–C and O–Cu–O (Table 2) fall in the range typical for similar "paddlewheel" copper complexes.[16] Two *p*-PyV ligands are coordinated through the nitrogen atoms of pyridyl substituents to the copper acetate core $[Cu_2(OCOCH_3)_4]$ in apical positions [$d_{Cu1–N5}$ = 2.206(4) and 2.179(4) Å for A and B, respectively]. Each copper ion is located in a distorted square-pyramidal coordination environment of four oxygen atoms from four acetate anions and one nitrogen atom in the apical position; the copper ions are located 0.217(2) and 0.206(2) Å above the oxygen square planes in complexes A and B, respectively. The N–N distances in the heterocyclic ring of the verdazyl ligand in $[Cu_2(OCOCH_3)_4(p\text{-PyV})_2]$ are very similar to those found for free *p*-PyV. The conformation of verdazyl in complex A is similar to that of free *p*-PyV [C19A and C7A lie 0.5895(7) and 0.103(7) Å out of the plane of the four nitrogen atoms], whereas the verdazyl ring in complex B is less distorted [C19B and C7B lie 0.496(8) and 0.077(7) Å out of the plane]. Drastic changes are observed between the planes. For example, the angle between the phenyl Φ1 and pyridyl Py rings increases from 3.31(13)° for free *p*-PyV to 31.46(20)° for complex A. The geometries of the two complexes are also slightly different. Thus, complex A is almost perfectly linear while complex B is "S" shaped (Figure 4). The *p*-PyV ligands in complexes A and B alternate and stack above each other in the *a* direction, and the sp^3-hybridized C19(A and B) atoms provide

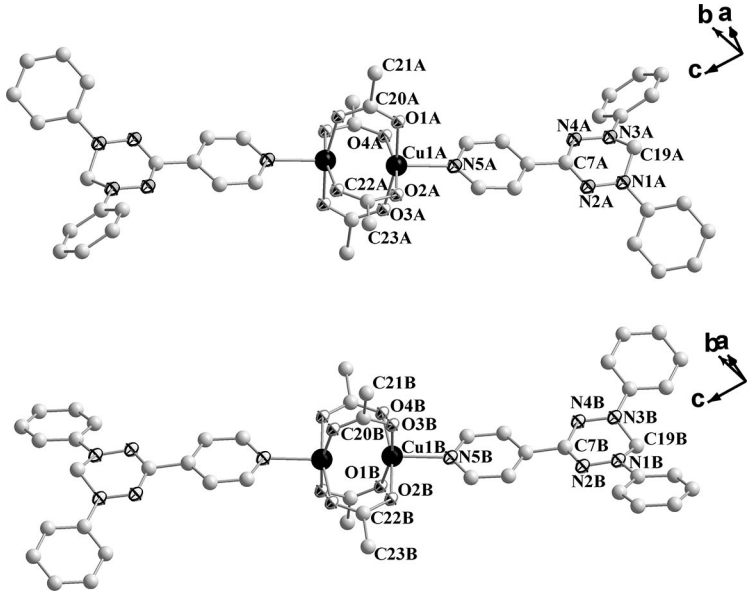

Figure 3. Molecular structures of the two molecules (top) A and (bottom) B. Hydrogen atoms have been omitted for clarity.

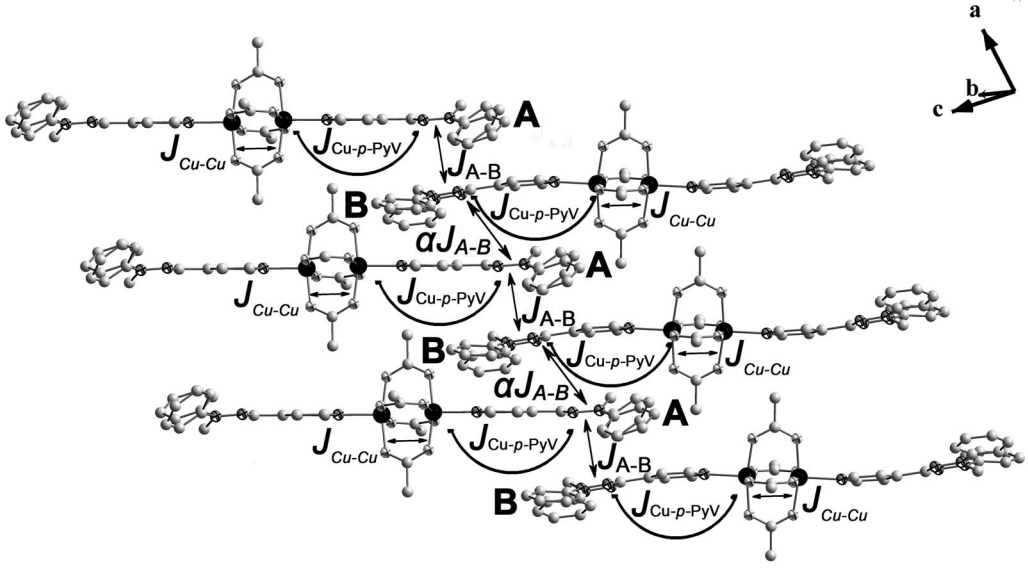

Figure 4. View of the dimers formed from complexes A and B along the *a* axis along with the coupling constants between local spins (see text).

interesting intermolecular interactions between complexes A and B: one hydrogen atom on C19A points toward the center of the pyridyl ring in complex B in a probable CH···π interaction [distance from H to mean square of Py ring: 3.964(1) Å], and one hydrogen atom on C19B is located at around 2.85 Å from N2A and N4A and therefore forms a weak hydrogen bond with these nitrogens. Complexes A and B are dimerized along the *a* direction. The verdazyl ligands of two molecules (B and A) are located above each other, with intermolecular distances between nitrogen atoms in the range between 3.754(3) ($d_{N4B–N1A}$) and 4.031(2) Å ($d_{N1B–N4A}$). The nitrogen atoms of the heterocyclic rings in A and B are more than 4.1 Å apart [the shortest being $d_{N4A–N2B}$ = 4.091(6) Å].

ESR Spectra

The ESR spectrum of *p*-PyV in toluene at room temperature consists of nine lines arising from coupling of the unpaired electron with the four nitrogen atoms of the heterocyclic ring. The values of *g* (2.008) and the nitrogen hyperfine splitting constant (6.82 G) are typical for verdazyl radicals.[5] No hyperfine structure was observed for the ESR spectrum of crystalline *p*-PyV at room temperature − the spectrum contains only one broad line (at g = 2.003). The absence of signal splitting in the solid state may be due to antiferromagnetic radical–radical interactions in the crystal lattice or by slow relaxation in the solid state.

The ESR spectrum of powdered $[Cu_2(OCOCH_3)_4(p\text{-}PyV)_2]$ at room temperature exhibits one very broad intense signal (half-width equal to 2500 G; g = 2.045) together with another, low-intensity signal at g = 2.003 consisting of nine not well-defined lines (a = 6.3 G). The signal at g = 2.045 can be assigned to the copper(II) ion − the presence of only one broad intense line with similar *g* values has been observed in the ESR spectra of some "paddle-wheel" copper(II) carboxylates.[17] The low-intensity signal at g = 2.003 in the ESR spectrum of $[Cu_2(OCOCH_3)_4(p\text{-}PyV)_2]$ can be assigned to coordinated *p*-PyV molecules not involved in magnetic coupling (see below). The difference (signal shape and hyperfine splitting) between the *p*-PyV signal in the spectrum of the complex and the spectrum of the free radical in toluene can be explained by the influence of *p*-PyV coordination to the copper(II) ion. Thus, coordination of *p*-PyV to copper(II) leads to a decrease of the electronic density on the heterocyclic ring, which results in a decrease in the hyperfine splitting constant in the coordinated radical compared to the free radical. Such changes upon coordination to a metal ion are common for the ESR spectra of metal-radical species.[12c,18]

Magnetic Properties

The temperature-dependence of the magnetization of a single crystal of *p*-PyV [186(±10) μg] was studied in the temperature range 2–300 K. As expected for organic radicals, the magnetization is independent of the crystal orientation and the results are presented for an arbitrary orientation. On cooling, χ_M increases smoothly and passes through a broad maximum located at T_{max} = 45 K then a minimum at 10 K (Figure 3). On cooling further, χ_M increases down to 2 K. The value of T_{max} observed for the single crystal of *p*-PyV is approximately six times lower than the bulk sample of *p*-PyV.[10] However, we assume these data to be more precise as they were obtained for a single crystal. The temperature dependence of χ_M can be reproduced with a dimer model ($H = -2J\,\boldsymbol{S_a}\cdot\boldsymbol{S_b}$) including non-coupled species (ρ).

$$\chi_M = \frac{Ng^2\beta^2}{kT\left(3+\exp\left(\frac{-2J}{kT}\right)\right)}(1-\rho)+\frac{Ng^2\beta^2}{kT}\rho$$

The best fit of the temperature-dependence of χ_M is represented in Figure 5 with the following parameters: J = –51.67(4) cm^{-1}, g = 1.917(1), ρ = 0.01610(7) [or 1.610(7)%] with $R_2 = \Sigma(\chi_{Mcalc} - \chi_{Mexp})^2/\Sigma(\chi_{Mexp})^2 = 2.89 \times 10^{-5}$. For comparison, we have added the experimental thermal variation of $\chi_M T$ to the curve calculated with the best fit parameters. Theory and experiment are in almost perfect agreement. The g value is smaller than that obtained by ESR due to the small error in the single-crystal mass measurement – a change of mass of 7 μg leads to a g value of 2.001(5), with almost identical values for other parameters. The distance between unpaired electrons, which are mainly located on the nitrogen atoms of verdazyl, within a pair is small enough to promote antiferromagnetic exchange between *p*-PyV molecules. Such behavior is typical for crystal lattices of verdazyl radicals. Antiferromagnetic coupling dominates in the majority of verdazyls,[19] although ferromagnetic coupling in the crystal lattices has been reported for radicals such as 3-(*p*-nitrophenyl)-1,5,6-triphenylverdazyl[7a] and 3-(*p*-cyanophenyl)-1,5-diphenyl-6-thioxoverdazyl.[7c] It was also found that even a small change in the inductive effects of the phenyl ring substituents leads to dramatic changes in the magnetic properties of verdazyls. Thus, 3-(*p*-bromophenyl)-1,5-dimethyl-6-thiooxoverdazyl behaves as a one-dimensional Heisenberg antiferromagnet, whereas 3-(*p*-chlorophenyl)-1,5-dimethyl-6-thiooxoverdazyl is a quasi-one-dimensional Heisenberg ferromagnet.[20] The magnitude of the interaction in *p*-PyV is moderate compared with that in other verdazyl derivatives.[19,21]

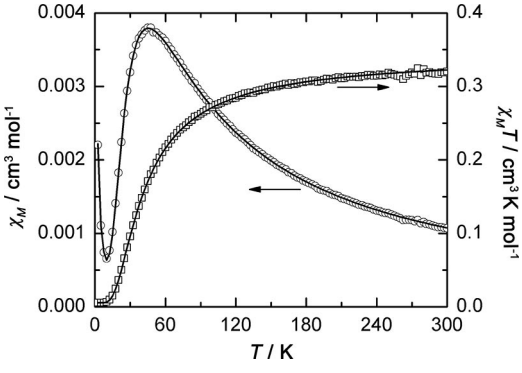

Figure 5. Temperature-dependence of χ_M and $\chi_M T$ for a single crystal of *p*-PyV. Experimental points are represented by white circles (χ_M) and white squares ($\chi_M T$) and the curves correspond to the best fits to the model described in the text (full lines).

The dependence of the magnetic susceptibility of $[Cu_2(OCOCH_3)_4(p\text{-PyV})_2]$ on temperature was studied in the temperature range between 2 and 300 K (Figure 6). At room temperature, $\chi_M T$ is equal to 1.12 cm^3 K mol^{-1}, much lower than expected for four non-interacting spins 1/2, two with a Zeeman factor ($g_{p\text{-}PyV}$) of 2.003 (the two radicals) and two with a Zeeman factor (g_{Cu}) of 2.045 [the two copper(II) ions, 1.574 cm^3 K mol^{-1}). On cooling, $\chi_M T$ decreases continuously, but with three slope changes at 145, 98, and 24 K, down to 0.047 cm^3 K mol^{-1} at 2 K. χ_M increases on cooling from room temperature, passes through a rounded maximum at T_{max} = 36 K, decreases down to 13 K, and then increases again on further cooling.

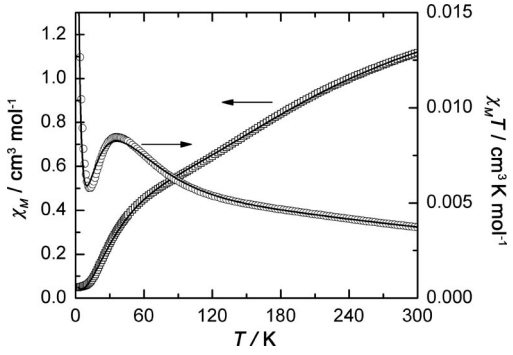

Figure 6. Temperature-dependence of χ_M and $\chi_M T$ for a powdered sample of $[Cu_2(OCOCH_3)_4(p\text{-PyV})_2]$. Experimental points are represented by white circles (χ_M) and white squares ($\chi_M T$) and the curves correspond to the best fits to the model described in the text (full lines).

The Curie tail below 13 K is clearly due to paramagnetic impurities resulting from partial decomposition and/or sample contamination. Some impurity is likely to arise due to intramolecular redox reactions, especially oxidation of *p*-PyV by Cu^{2+}, which leads to the formation of uncoupled Cu^{2+} ion and uncoupled *p*-PyV radical (ESR signal at g = 2.003, see above). Bearing in mind the similar values of the redox potentials of Cu^{2+} and verdazyls,[22] such a supposition seems to be reasonable (a direct comparison of $E_{1/2}$ values makes no sense as these potentials are measured in solution and depend on certain coordination environments).

The following superexchange interactions may be expected between spins 1/2 on the basis of an analysis of the crystal structure of $[Cu_2(OCOCH_3)_4(p\text{-PyV})_2]$: i) intramolecular coupling between the spins of copper(II) atoms through acetates (Cu^{II}-Cu^{II}), which is always observed in "paddle-wheel" dimeric copper complexes;[11] ii) intramolecular coupling between the spins of the copper ion and *p*-PyV through the pyridyl ring (Cu^{II}–*p*-PyV); and iii) intermolecular coupling between the *p*-PyV fragments of adjacent complexes A and B. In principle, since there are two crystallographically independent complexes there should be two different Cu^{II}-Cu^{II} and Cu^{II}-*p*-PyV superexchange interactions. However, in order to avoid overparametrization we have kept only one Cu^{II}-Cu^{II} interaction. Likewise, the coupling between Cu^{II} spins and verdazyl radicals is expected to be very small with respect to the coupling between Cu^{II} spins. The magnetic $d_{x^2-y^2}$ orbital of Cu^{II} lies in the CuO_4 plane (where O are oxygen atoms of acetates) and therefore the spin density of the unpaired electron along the Cu1–N5 bond is very small, which minimizes the coupling with verdazyls. The coupling parameters $J_{Cu\text{-}Cu}$, $J_{A\text{-}B}$, and $J_{B\text{-}A}$ can therefore be considered. The following in-field Hamiltonian can be written on the basis of the coupling scheme shown in Figure 4.

$$H = \sum_{i=1}^{n} \begin{pmatrix} -J_{A-B}\left(S_{Ai} \cdot S_{Bi} + \alpha S_{Bi} \cdot S_{Ai+1}\right) \\ -J_{Cu-Cu}\left(S_{Cu1\,Ai} \cdot S_{Cu2\,Ai} + S_{Cu1\,Bi} \cdot S_{Cu2\,Bi}\right) \\ + g_{p-PyV}\beta H \cdot S_{Ai} + g_{p-PyV}\beta H \cdot S_{Bi} \\ + g_{Cu}\beta H \cdot S_{Cu1\,Ai} + g_{Cu}\beta H \cdot S_{Cu1\,Bi} \end{pmatrix}$$

where S_{Ai} and S_{Bi} are the spin operators associated with verdazyl radicals on complexes A and B at site *i*, S_{Cu} is the spin operator of the Cu^{II} spins on complexes A and B, $g_{p\text{-PyV}}$ and g_{Cu} the Zeeman factors associated with Cu^{II} and verdazyl spins, $J_{A\text{-}B}$ and $\alpha J_{A\text{-}B}$ are the coupling constants between radicals in a chain along *a*, and $J_{Cu\text{-}Cu}$ the coupling constant between Cu^{II} spins. There is no coupling between organic (verdazyls alternating chain) and inorganic networks (Cu^{II} dimers), so the mathematical expressions for the thermal dependence of the magnetic susceptibilities of the two networks ($\chi_{p\text{-PyV}}$ and χ_{Cu}) can be derived separately.[23] Hatfield has proposed an expression for $\chi_{p\text{-PyV}}$ vs. *T* using the ring chain method[24]

$$\chi_M = (1-\rho)(\chi_{Cu} + \chi_{p-PyV}) + \rho\frac{N\beta^2}{kT}\left(\frac{g^2{}_{Cu} + g^2{}_{p-PyV}}{2}\right)$$

$$\chi_{Cu} = \frac{2N\beta^2 g^2{}_{Cu}}{kT\left(3 + \exp\left(\frac{-J_{Cu-Cu}}{kT}\right)\right)}$$

$$\chi_{p-PyV} = \frac{2N\beta^2 g^2{}_{p-PyV}}{kT}\frac{A + Bx + Cx^2}{1 + Dx + Ex^2 + Fx^3}$$

$$\text{with } x = \frac{\left|J_{A-B}\right|}{kT}$$

where *N*, β, and *k* have their standard meanings and ρ is the percentage of paramagnetic impurities. The above expression is valid for negative $J_{A\text{-}B}$ and for $0 \le \alpha \le 1$. The A–F coefficients are functions of α and two sets of coefficients have been proposed for $0 \le \alpha \le 0.4$ and $0.4 \le \alpha \le 1$.[23] The best agreement with experimental $\chi_M T$ vs. *T* data has been unambiguously obtained for $\alpha > 0.4$ with $g_{p\text{-PyV}} = 2.00$ fixed with the following parameters: $J_{Cu\text{-}Cu} = -359(2)$ cm^{-1}, $J_{A\text{-}B} = -52.0(3)$ cm^{-1}, $g_{Cu} = 2.20(1)$, $\alpha = 0.59(1)$, and $\rho = 3.94(9)\%$, with $R_2 = \Sigma(\chi_M T_{calc} - \chi_M T_{exp})^2/\Sigma(\chi_M T_{exp})^2 = 5.59 \times 10^{-5}$ (see Figure 6). The calculated χ_M vs. *T* curve with this set of parameters is also shown in Figure 6. Considering the excellent agreement between theory and experiment we can say that if an interaction exists between verdazyl and copper its magnitude is much weaker than for the other interactions and is therefore undetectable.

The magnitude of $J_{Cu\text{-}Cu}$ is close to values observed for "paddle-wheel" copper complexes with pyridine substituents[25] and to the values observed for copper acetate complexes with pyridine nitronyl nitroxides in apical positions.[12b,12c,26] No interaction between nitronyl nitroxide and copper(II) ion was observed for these compounds, similarly to $[Cu_2(OCOCH_3)_4(p\text{-PyV})_2]$, which was also explained by the absence of unpaired electron density on the orbitals involved in copper-radical bond formation. A dependence of the nature and magnitude of the superexchange interaction on the type of magnetic orbitals involved in copper(II)-radical bond formation has also been found for other copper(II) verdazyl complexes. Thus, equatorial coordination of 1,5-dimethyl-3-(2-pyridyl)-6-oxoverdazyl (*o*-PyVerd) to copper(II) ion in $[CuCl_2(o\text{-PyVerd})(H_2O)]$ results in a strongly antiferromagnetic exchange between Cu^{II} and the radical, while axial bounding of 1,5-dimethyl-3-(*N*-methyl-2-imidazolyl)-6-oxoverdazyl (ImVerd) to Cu^{II} in $[Cu(hfac)_2(ImVerd)]$ leads to weak ferromagnetic exchange.[27] However, the nitrogen atom of the heterocyclic ring on which unpaired electron density is mostly localized coordinates directly to copper(II) ion in these complexes, while in $[Cu_2(OCOCH_3)_4(p\text{-PyV})_2]$ this atom is separated from the metal ion by a pyridyl ring. Thus, binding of verdazyl to Cu ions through a pyridine ring results in almost zero interaction between the unpaired electron of verdazyl and the unpaired electrons of Cu^{II}.

The nature and the magnitude of the exchange interaction between verdazyl radicals in $[Cu_2(OCOCH_3)_4(p\text{-PyV})_2]$ ($J_{A\text{-}B}$) is surprisingly equal to the exchange interaction in *p*-PyV. This can only be a coincidence because the overlaps between radicals in the two crystal structures are very different. Furthermore, in the model described above we have considered that the stronger interaction between radicals ($J_{A\text{-}B}$) coincides with the shorter intermolecular distances between nitrogen atoms. As a matter of fact, the analytical expression of χ_M vs. *T* would be rigorously identical if the roles of $J_{A\text{-}B}$ and $\alpha J_{A\text{-}B}$ were inverted. It is beyond the scope of this paper to ascribe exchange interactions to the packing of verdazyl radicals. However, we can say that our set of parameters is not unrealistic with the exchange interaction between close radicals being stronger than between radicals which are more distant. Any attempts to fit the data considering that one of the intermolecular verdazyl–verdazyl exchange interactions is negligible with respect to the other, in other words to consider verdazyl dimers, leads to poor agreement, which can only be improved by incorporating a large temperature-independent paramagnetism, which is meaningless.

Conclusions

The crystal structure and spectral and magnetic properties of 3-(*p*-pyridyl)-1,5-diphenylverdazyl (*p*-PyV) and its complex $[Cu_2(OCOCH_3)_4(p\text{-PyV})_2]$ have been studied. An analysis of the structural and magnetic behavior of *p*-PyV has revealed the existence of antiferromagnetic interactions [$J = -51.67(4)$ cm^{-1}] between two neighboring *p*-PyV molecules in the radical crystal lattice. No signs of the spin frustration suggested earlier for *p*-PyV[10] have been found. This difference between the magnetic properties described here and those reported by Mukai et al.[10] is likely to be a result of the different crystal structures (for example, different modifications) of the *p*-PyV samples studied. This may result from the different purification procedures used by Mukai et al. and by us. It is well known[28] that different synthetic methods can lead to different crystal phases of the

same substance, which can sometimes exhibit different magnetic properties.[29]

$[Cu_2(OCOCH_3)_4(p\text{-PyV})_2]$ belongs to the "paddle wheel" family of copper complexes with the pyridine-substituted verdazyl radicals in the axial position. The crystal structure shows alternating organic chains covalently linked to copper dimers. No interaction between verdazyls and copper has been detected between the organic and inorganic magnetic networks. Copper-verdazyl coupling in this complex is negligibly small, which may be explained by the absence of unpaired electron density on the d_{z^2} orbital of copper(II) involved in Cu–N bond formation. The magnetization measurements for $[Cu_2(OCOCH_3)_4(p\text{-PyV})_2]$ can be reproduced with a Heisenberg AFM/AFM alternating linear chain model for the organic network and a simple singlet-triplet equilibrium for copper dimers.

Experimental Section

General: Commercially available reagents and solvents (Merck) were used as received. *p*-PyV was synthesized as described previously[10] and was additionally purified by multiple crystallization from toluene by layering with hexane. C,H,N content was determined with a Carlo Erba 1106 CHN analyser. ESR spectra were recorded using a PS 100.X spectrometer. Magnetic measurements were performed with a Quantum Design MPMS SQUID magnetometer operating in the temperature range 2–300 K with a DC magnetic field of up to 5 T. The single crystal of *p*-PyV used for magnetic measurements was about $0.2 \times 0.2 \times 0.1$ mm in size and was checked by X-ray diffraction before measurement of the cell parameters; the purity of the sample from which the crystal was selected was also confirmed by elemental analysis.

Synthesis of $[Cu_2(OCOCH_3)_4(p\text{-PyV})_2]$: $[Cu_2(OCOCH_3)_4(H_2O)_2]$ (0.4 g, 1 mmol) was dissolved in a methanol solution (10 mL) of *p*-PyV (0.628 g, 2 mmol). After 30 min, green crystals of $[Cu_2(OCOCH_3)_4(p\text{-PyV})_2]$ suitable for X-ray diffraction were separated from the reaction mixture. Yield 64%. Elemental analysis for $C_{46}H_{44}Cu_2N_{10}O_8$ (992.01): calcd. C 55.70, H 4.47, N 14.12; found C 55.31, H ,4.51 N 14.02.

Crystallographic Data Collection and Structure Determination: Single crystals of the title compounds were mounted on a Nonius four-circle diffractometer equipped with a CCD camera and a graphite-monochromated Mo-K_α radiation source (λ = 0.71073 Å) at the Center de Diffractométrie (CDFIX), Université de Rennes 1, France. The structures of *p*-PyV and $[Cu_2(OCOCH_3)_4(p\text{-PyV})_2]$ were solved by direct methods using SHELXS-97[30] software, and were refined with full-matrix least-squares method on F^2 using SHELXL-97.[30] Hydrogen atoms were placed at calculated positions and refined using a riding model. Crystallographic data are summarized in Table 3.

Table 3. Crystallographic data.

	p-PyV	$[Cu_2(OCOCH_3)_4(p\text{-PyV})_2]$
Chemical formula	$C_{19}N_5H_{16}$	$Cu_2C_{46}N_{10}O_8H_{44}$
Formula weight	314.37	991.99
Crystal system	monoclinic	triclinic
Space group	$P2_1/c$ (no. 14)	$P\bar{1}$ (no. 2)
a [Å]	9.4648(4)	8.3133(3)
b [Å]	16.0588(6)	10.8032(4)
c [Å]	10.9723(5)	26.5746(10)
α [°]	90.	78.4126(10)
β [°]	109.6389(19)	81.9789(12)
γ [°]	90.	77.4517(14)
V [Å^3]	1570.70(11)	2270.68(15)
Z	4	2
Calcd. density [g cm^{-3}]	1.329	1.451
Total/unique reflections	8185/4943	13718/7992
Reflections $I > 2\sigma(I)$	1937	4118
R_1 [for $I > 2\sigma(I)$]	0.0620	0.0590

CCDC-686542 (for *p*-PyV) and -686543 (for $[Cu_2(OCOCH_3)_4(p\text{-PyV})_2]$) contain the supplementary crystallographic data for this paper. These data can be obtained free of charge from The Cambridge Crystallographic Data Center via www.ccdc.cam.ac.uk/data_request/cif.

[1] a) A. Caneschi, D. Gatteschi, P. Rey, *Prog. Inorg. Chem.* **1991**, *39*, 331–429; b) D. Luneau, P. Rey, *Coord. Chem. Rev.* **2005**, *249*, 2591–2611; c) A. Caneschi, D. Gatteschi, N. Lalioti, C. Sangregorio, R. Sessoli, G. Venturi, A. Vindigni, A. Rettori, M. G. Pini, M. A. Novak, *Angew. Chem. Int. Ed.* **2001**, *40*, 1760–1763; d) L. Bogani, C. Sangregorio, R. Sessoli, D. Gatteschi, *Angew. Chem. Int. Ed.* **2005**, *44*, 5817–5821; e) K. Bernot, L. Bogani, A. Caneschi, D. Gatteschi, R. Sessoli, *J. Am. Chem. Soc.* **2006**, *128*, 7947–7956; f) K. Inoue, T. Hayamizu, H. Iwamura, D. Hashizume, Y. Ohashi, *J. Am. Chem. Soc.* **1996**, *118*, 1803–1804; g) T. Ise, T. Ischida, D. Hashizume, F. Iwasaki, T. Nogami, *Inorg. Chem.* **2003**, *42*, 6106–6113.

[2] a) H. Oshio, T. Watanabe, A. Ohto, T. Ito, U. Nagashima, *Angew. Chem. Int. Ed. Engl.* **1994**, *33*, 670–671; b) V. Laget, C. Hornick, P. Rabu, M. Drillon, P. Turek, R. Ziessel, *Adv. Mater.* **1998**, *10*, 1024–1028; c) H. Oshio, M. Yamamoto, N. Hoshino, T. Ito, *Polyhedron* **2001**, *20*, 1621–1625; d) N. Mihara, Y. Teki, *Polyhedron* **2007**, *26*, 2142–2146.

[3] a) D. A. Shultz, S. H. Bodnar, *Inorg. Chem.* **1999**, *38*, 591–594; b) D. A. Shultz, S. H. Bodnar, K. E. Vostrikova, J. W. Kampf, *Inorg. Chem.* **2000**, *39*, 6091–6093; c) D. A. Shultz, J. C. Sloop, T. A. Coote, M. Beikmohammadi, J. Kampf, P. D. Boyle, *Inorg. Chem.* **2007**, *46*, 273–277; d) S. Bruni, A. Caneschi, F. Cariati, C. Delfs, A. Dei, D. Gatteschi, *J. Am. Chem. Soc.* **1994**, *116*, 1388–1394.

[4] a) M. Tamura, Y. Nakazawa, D. Shiomi, K. Nozawa, Y. Hosokoshi, M. Ishikawa, M. Takahashi, M. Kinoshita, *Chem. Phys. Lett.* **1991**, *186*, 401–404; b) R. Chiarelli, M. A. Novak, A. Rassat, J. L. Tholence, *Nature* **1993**, *363*, 147–149; c) R. Imachi, T. Ishida, T. Nogami, S. Ohira, K. Nishiyama, K. Nagamine, *Chem. Lett.* **1997**, *3*, 233–234.

[5] a) F. A. Neugebauer, H. Fischer, R. Siegel, *Chem. Ber.* **1988**, *121*, 812–822; b) F. A. Neugebauer, H. Fischer, C. Krieger, *J. Chem. Soc. Perkin Trans. II* **1993**, *2*, 535–544; c) C. L. Barr, P. A. Chase, R. G. Hicks, M. T. Lemaire, C. L. Stevens, *J. Org. Chem.* **1999**, *64*, 8893–8897; d) M. Chahma, K. Macnamara, A. van der Est, A. Alberola, V. Polo, M. Pilkington, *New J. Chem.* **2007**, *31*, 1973–1978; e) J. B. Gilroy, S. D. J. McKinnon, B. D. Koivisto, R. G. Hicks, *Org. Lett.* **2007**, *9*, 4837–4840.

[6] a) R. G. Hicks, *Aust. J. Chem.* **2001**, *54*, 597–600; b) B. D. Koivisto, R. G. Hicks, *Coord. Chem. Rev.* **2005**, *249*, 2612–2630; c) K. Nakabayashi, Y. Ozaki, M. Kawano, M. Fujita, *Angew. Chem. Int. Ed.* **2008**, *47*, 2046–2048; d) M. Lemaire, T. M. Barclay, L. K. Thompson, R. G. Hicks, *Inorg. Chim. Acta* **2006**, *359*, 2616–2621.

[7] a) P. M. Allemand, G. Srdanov, F. Wudl, *J. Am. Chem. Soc.* **1990**, *112*, 9391–9392; b) R. K. Kremer, B. Kanellakopulos, P. Bele, H. Brunner, F. A. Neugebauer, *Chem. Phys. Lett.* **1994**, *230*, 255–258; c) K. Mukai, M. Nuwa, T. Morishita, T. Muramatsu, T. C. Kobayashi, K. Amaya, *Chem. Phys. Lett.* **1997**, *272*, 501–505.

[8] R. G. Hicks, B. D. Koivisto, M. T. Lemaire, *Org. Lett.* **2004**, *6*, 1887–1890.

[9] R. G. Hicks, M. T. Lemaire, L. K. Thompson, T. M. Barclay, *J. Am. Chem. Soc.* **2000**, *122*, 8077–8078.
[10] K. Mukai, M. Matsubara, H. Hisatou, Y. Hosokoshi, K. Inoue, N. Azuma, *J. Phys. Chem. B* **2002**, *106*, 8632–8638.
[11] M. Kato, Y. Muto, *Coord. Chem. Rev.* **1988**, *92*, 45–83.
[12] a) U. Schatzschneider, T. Weyhermüller, E. Rentschler, *Inorg. Chim. Acta* **2002**, *337*, 122–130; b) I. Dasna, S. Golhen, L. Ouahab, O. Peña, N. Daro, J.-P. Sutter, *New J. Chem.* **2000**, *24*, 903–906; c) R. E. D. Rico, A. M. Arif, J. S. Miller, *Inorg. Chem.* **2000**, *39*, 4894–4902.
[13] N. Azuma, *Bull. Chem. Soc. Jpn.* **1982**, *55*, 1357–1361.
[14] C. Janiak, *J. Chem. Soc., Dalton Trans.* **2000**, 3885–3896.
[15] J. N. van Niekerk, F. R. L. Schoening, *Acta Crystallogr.* **1953**, *6*, 227–232.
[16] a) D. E. Williams, *Acta Crystallogr., Sect. B* **1973**, *29*, 96–102; b) M. Yamanaka, H. Uekusa, S. Ohba, Y. Saito, S. Iwata, *Acta Crystallogr., Sect. B* **1992**, *48*, 650–653.
[17] a) M. Kato, Y. Muto, *Coord. Chem. Rev.* **1988**, *92*, 45–83; b) F. Cariati, L. Erre, G. Micera, L. Menabue, M. Saladini, P. Prampolini, *Inorg. Chim. Acta* **1982**, *63*, 85–89.
[18] A. V. Yakovenko, S. V. Kolotilov, A. W. Addison, S. Trofimenko, G. P. A. Yap, V. Lopushanskaya, V. V. Pavlishchuk, *Inorg. Chem. Commun.* **2005**, *8*, 932–935.
[19] a) K. Mukai, S. Kawasaki, J. B. Jamali, N. Achiwa, *Chem. Phys. Lett.* **1995**, *241*, 618–622; b) K. Mukai, K. Konishi, K. Nedachi, K. Takeda, *J. Magn. Magn. Mater.* **1995**, *140–144*, 1449–1450.
[20] K. Mukai, K. Konishi, K. Nedachi, K. Takeda, *J. Phys. Chem. B* **1996**, *100*, 9658–9663.
[21] K. Mukai, M. Nuwa, K. Suzuki, S. Nagaoka, N. Achiwa, J. B. Jamali, *J. Phys. Chem. B* **1998**, *102*, 782–787.
[22] a) I. Bernal, *Stereochemical Control, Bonding and Steric Rearrangements*, Elsevier, Amsterdam, **1990**; b) O. Polumbrik, *Chemistry of Verdazyl Radicals*, Naukova Dumka, Kiev, **1984**.
[23] O. Kahn, *Molecular Magnetism*, VCH Publishers, New York, **1993**.
[24] J. W. Hall, W. E. Marsh, R. R. Weller, W. E. Hatfield, *Inorg. Chem.* **1981**, *20*, 1033–1037.
[25] Y. Muto, T. Toku, K. Chijiwa, M. Kato, *Bull. Chem. Soc. Jpn.* **1984**, *57*, 1008–1011.
[26] Y.-H. Chung, H.-H. Wei, G.-H. Lee, Y. Wang, *Inorg. Chim. Acta* **1999**, *293*, 30–36.
[27] J. B. Gilroy, B. D. Koivisto, R. McDonald, M. J. Ferguson, R. G. Hicks, *J. Mater. Chem.* **2006**, *16*, 2618–2624.
[28] a) A. Zakrassov, V. Shteiman, Y. Sheynin, M. Botoshansky, M. Kapon, M. Kaftory, R. E. Del Sesto, J. S. Miller, *Helv. Chim. Acta* **2003**, *86*, 1234–1245; b) K. S. Gavrilenko, S. V. Punin, O. Cador, S. Golhen, L. Ouahab, V. V. Pavlishchuk, *J. Am. Chem. Soc.* **2005**, *127*, 12246–12253.
[29] a) K. S. Gavrilenko, O. Cador, K. Bernot, P. Rosa, R. Sessoli, S. Golhen, V. V. Pavlishchuk, L. Ouahab, *Chem. Eur. J.* **2008**, *14*, 2034–2043; b) M. Kinoshita, *Jpn. J. Appl. Phys.* **1994**, *33*, 5718–5733.
[30] G. M. Sheldrick, *SHELX-97*, University of Göttingen, Germany, **1997**.

Received: January 2, 2009
Published Online: April 28, 2009

